The Sensitivity of Actuator-Disc RANS Simulations to Turbulence Length Scale Assumptions

T. Blackmore[#1], W.M.J. Batten[#], M.E. Harrison[#], A.S. Bahaj[#]

[#]*Sustainable Energy Research Group, School of Civil Engineering and the Environment, University of Southampton, Southampton, SO17 1BJ, UK*

[1]T.Blackmore@soton.ac.uk

***Abstract*— It has previously been shown that ambient turbulence affects the results from computational fluid dynamics (CFD) models when using an actuator disc to simulate marine current turbines. The turbulence parameters are often estimated using an empirical equation that is dependent on a turbulence length scale. In most literature this length scale is commonly highlighted as the authors 'best guess' with little scientific reasoning. The work presented here investigates the effects of using different length scales on the development of a flow in a circulating water channel. The results showed that the best agreement is achieved with a length scale of one third the channel depth. The obtained turbulence parameters were then used with an actuator disc model. Agreement with experimental data was initially poor as the velocity deficit was severely under predicted. The addition of a turbulence source at the disc improved the agreement with experimental data significantly. It was found that the length scale of the disc turbulence should be the diameter of the holes used on the porous discs for experiments. However, there were still discrepancies between the experimental and model turbulence intensities. A possible cause of this may be that the turbulence intensity added at the disc was under predicted. Further work is needed to establish if better agreement can be achieved by increasing the turbulence at the disc.**

***Keywords*— Actuator disc, RANS, CFD, Turbulence, OpenFOAM.**

I. INTRODUCTION

Solution of the Reynolds Averaged Navier Stokes (RANS) equations incorporating an actuator disc to model wind turbines has been widely used due to the computational efficiency and reasonable agreement with experimental data [1, 2].

The actuator disc has the same geometry as the swept area of the turbine and approximates the forces applied to the surrounding flow. The forces are incorporated into the discretised RANS equations though the inclusion of a negative momentum source term. Turbulence modelling is often carried out using the k-ε model, again due to its computational efficiency. The turbulence is described by the turbulent kinetic energy, k, and the turbulence dissipation rate, ε [3].

The effects of ambient turbulence intensity on the turbine wake have been shown to be significant by Sun [4] and MacLeod [5]. Increasing the ambient turbulence intensity increases the mixing in the wake due to increased velocity fluctuations. This increase in mixing between the free stream and turbine wake results in higher momentum fluid entering the wake region causing the velocity deficit to recover to free stream faster [6].

Model inlet conditions of turbulent kinetic energy can be calculated directly from measured turbulence intensities. However, the inlet values of turbulence dissipation are based on an empirical expression that is dependent on a turbulence length scale, which is not easy to measure experimentally. Inlet conditions for turbulence dissipation are therefore often based on the author's 'best-guess' of what the turbulence length scale might be. Harrison *et al* [7] took the length scale to be the channel depth and Sun [4] took the length scale to be 0.07 times the hydraulic diameter. More complex approximations for the length scale exist based on functions relating the length scale to the wall proximity and some other length as shown in Veesteeg & Malalasekera [3]. There are many options for the length scale but as mentioned previously the ambient turbulence intensity affects the wake. It is therefore likely that the length scale chosen will affect the results.

This study investigates the effects of the length scale on the ambient turbulence in a channel, and considers how this effects the development of the flow.

It also considers the effect of turbulent source terms at the disc by adding values of turbulent kinetic energy and turbulence dissipation at the disc location to simulate the turbulence generated by a turbine. Roc *et al*, [8] showed that the addition of a turbulence source term significantly improved the agreement to experimental data for the k-ω turbulence model.

The validity of the approach is considered by comparing to experimental data from a comprehensive experimental programme carried out at the University of Southampton, [6].

II. THEORY

An incompressible RANS solver was used to solve the three dimensional Reynolds-averaged mass and momentum conservation equations.

Mass conservation:

$$\nabla . U = 0 \tag{1}$$

Momentum conservation:

$$\nabla . (UU) - \nabla . (\nu_{eff} \nabla U) - \nabla . \{\nu_{eff} dev[(\nabla U)^T]\} = -\nabla \left(\frac{p}{\rho}\right) + S \tag{2}$$

Where U is the time averaged velocity, ν_{eff} is the effective viscosity (the sum of viscosity and turbulent viscosity), p is the pressure, ρ is the density, S is an added source term, $(\nabla U)^T$ is the transpose of (∇U), and $dev[(\nabla U)^T]$ is the deviatoric component of $(\nabla U)^T$.

A. Ambient Turbulence

The *k-ε* turbulence model was chosen due to its computational efficiency and proven application over a wide range of flows [3]. The turbulence is defined through two parameters; the turbulent kinetic energy and the turbulence dissipation requiring two extra transport equations to be solved.

$$\frac{\partial k}{\partial t} + \nabla . \Phi k - \nabla . (\nu_{eff} \nabla \mathrm{k}) = 2\nu_t E_{ij} E_{ij} - \varepsilon \tag{3}$$

$$\frac{\partial \varepsilon}{\partial t} + \nabla . \Phi \varepsilon - \nabla . (\nu_{eff} \nabla \varepsilon) = C_{1\varepsilon} \frac{\varepsilon}{k} 2\nu_t E_{ij} E_{ij} - C_{2\varepsilon} \frac{\varepsilon^2}{k} \tag{4}$$

Where ν_t is the turbulent viscosity, Φ is the transport quantity - velocity, $C_{1\varepsilon}$ and $C_{2\varepsilon}$ are constants, and Eij is the mean rate of deformation of a fluid element.

Boundary and inlet values are required for the turbulent kinetic energy and the turbulence dissipation to provide closure to their transport equations. Inlet values for the turbulent kinetic energy can be calculated directly from measured turbulence intensities using Equation 5.

$$k = \frac{3}{2} I^2 U^2 \tag{5}$$

Where I is the turbulence intensity.

However, inlet values for turbulence dissipation are evaluated using Equation 6 which contains empirical values. There is therefore some uncertainty in the turbulence dissipation.

$$\varepsilon_i = C_\mu^{3/4} \frac{k^{3/2}}{\ell_i} \tag{6}$$

Where: C_μ is a dimensionless constant, equal to 0.09 and ℓ_i is the turbulence length scale.

The length scale can be taken as a constant value based on some domain geometry or as a function, Equation 7, based on the distance from a wall, *y*, and some other length, *f*, as shown in Versteeg & Malalasekera [3].

$$\ell_f = f\left[0.14 - 0.08\left(1 - \frac{y}{f}\right)^2 - 0.06\left(1 - \frac{y}{f}\right)^4\right] \tag{7}$$

Different estimates for the length scale have been used as shown in Table 1.

TABLE 1
LENGTH SCALES USED FOR AMBIENT TURBULENCE INVESTIGATION

Turbulent Length Scale, ℓ_i
ℓ_w = channel width
$\ell_{w/2}$ = half channel width
ℓ_d = channel depth
$\ell_{d/3}$ = third channel depth
$\ell_{f=d}$: f= channel depth
$\ell_{f=w/2}$: f= half channel width

B. Actuator Disc Model

The RANS actuator disc model simulates a turbine by including a momentum sink term in the region the turbine is located. This simulates the effects a turbine would have on the flow field without the need to directly model the turbine. Modelling the turbine directly would require a much finer mesh and therefore a significant increase in computational resources. The source term is only applied in the disc region and described in the next section.

1) Momentum Source Term, S: The source term is calculated using actuator disc momentum theory and the term is defined such that the thrust and power coefficients of the disc will be similar to that of the actual turbine being modelled.

$$C_T = \frac{T}{\frac{1}{2}\rho U^2 A} \tag{8}$$

$$C_P = \frac{P}{\frac{1}{2}\rho U^3 A} \tag{9}$$

$$a = 1 - \frac{C_T}{C_P} \tag{10}$$

$$C_T = 4a(1-a) \tag{11}$$

$$U_t = U(1-a) \tag{12}$$

$$T = 2\rho A U^2 a(1-a) = 2\rho A |U_1| \frac{a}{(1-a)} . U_1 \tag{13}$$

Where T is thrust, C_T is the thrust coefficient, P is power, C_P is the power coefficient, A is the disc area, a is the axial induction factor, U_1 is the velocity at the disc, and U is the free stream velocity [1]. C_T and C_P were set to 0.86 and 0.58 respectively for all model simulations with a disc corresponding to the values recorded for the experimental work.

Dividing by the total disc volume, V_{Tot}, gives the force per unit volume and introducing a tensor, E, to define the direction the source term acts in yields Equation 14.

$$\frac{T}{V_{Tot}} = \frac{1}{V_{Tot}} 2\rho A |U_1| \frac{a}{(1-a)} . E . U_1 \tag{14}$$

Finally, dividing by density, for incompressible flow, results in the source term, S, as shown in Equation 15.

$$S = \frac{2A}{V_{Tot}}|U_1|\frac{a}{(1-a)}.E.U_1 \quad (15)$$

2) *Actuator Disc Turbulence Source:* To improve the realism of the actuator disc model a turbulence source can be added at the disc to account for the turbulence generated by the turbine. The maximum added turbulence intensity behind a turbine can be approximated using Equation 16 [9].

$$\Delta I_m = 0.725a = 0.362\left[1-(1-C_T)^{\frac{1}{2}}\right] \quad (16)$$

As for the ambient turbulence, the maximum added turbulent kinetic energy can be calculated using Equation 5, and the maximum added turbulence dissipation can be calculated using Equation 6. Two length scales were used; the diameter of the holes and half the diameter of the holes on the actuator disc used in experiments. The turbulent kinetic energy and turbulence dissipation were set to these maximum values at each discrete region within the actuator disc.

III. METHODOLOGY

A. *Experimental Method*

Experiments were performed in a circulating water channel measuring 21m in length, 1.37m wide, and at a water depth of 0.3m located at the University of Southampton. Porous discs of 0.1m diameter were used to simulate the presents of a turbine with a thrust coefficient of 0.86. Thrust was measured using a load cell and upstream and downstream velocities were measured using an acoustic Doppler velocimeter at a sample rate of 50Hz. Full details of the experimental procedure are presented in [6].

B. *Numerical Method*

Open source CFD software, OpenFOAM® 1.7.1 [10] was used to solve the RANS equations with the simpleWindFoam solver. The solver is for single phase, incompressible, steady state problems and uses the SIMPLE algorithm for pressure-velocity coupling. The solver allows actuator disc source terms to be included by defining a disc region and specifying thrust and power coefficients. Combinations of central differencing and van Leer TVD schemes were used for the discretisation of the equations. A preconditioned conjugate gradient solver for symmetric matrices, PCG, and a preconditioned bi-conjugate gradient solver for asymmetric matrices, PBiCG, were used to solve the discretised equation as they were found to produce a solution faster than the basic iterative method with the SmoothSolver [11].

C. *Inlet Values*

A velocity profile fitted to experimental data recorded for the inlet profile of the flume was used as the model inlet condition and described by Equation 17.

$$U = 2.5U^* ln\left(\frac{y_w U^*}{\nu}\right) + B \quad (17)$$

Where constant B = 0.197*m/s*, the friction velocity U^* = 0.00787*m/s*, y_w is the distance from the bed, and ν is the kinematic viscosity.

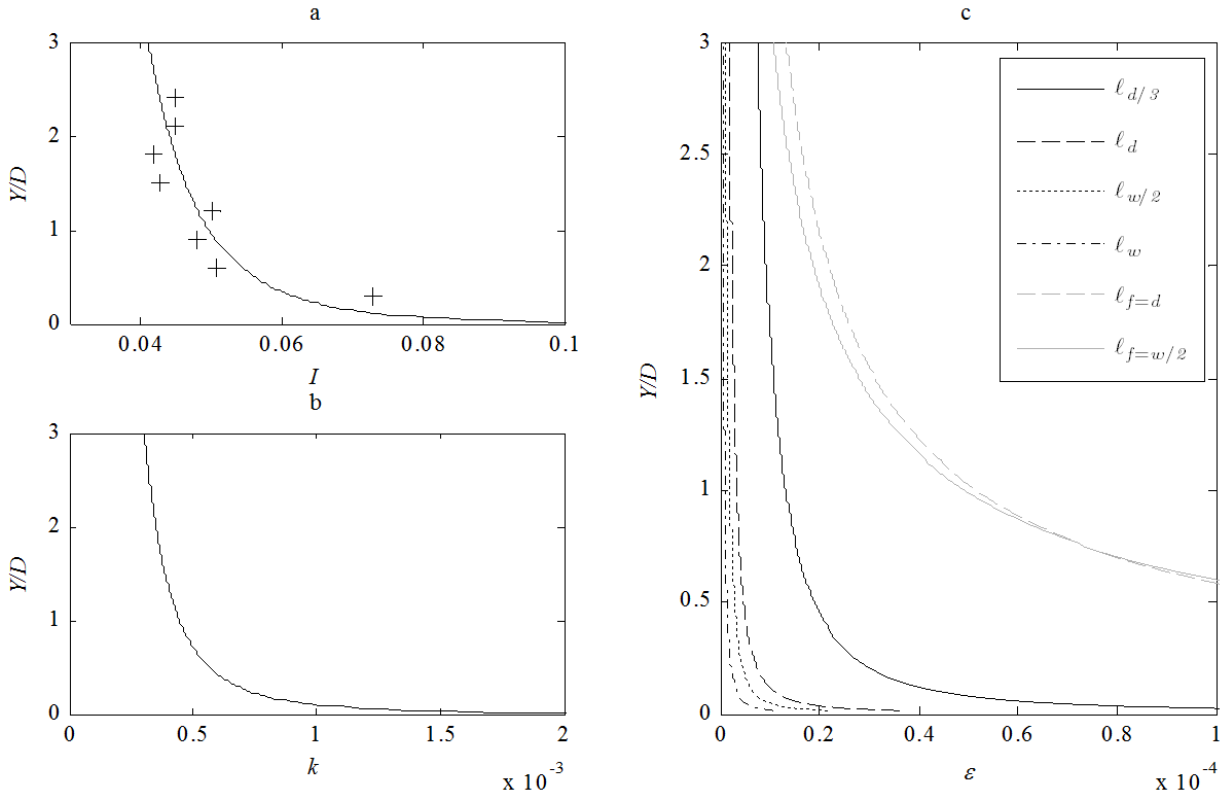

Figure 1 - Turbulence inlet parameters. a) turbulence intensity [crosses are experimental data, line is the fitted inlet profile, Equation 18], b) Turbulent kinetic energy, c) Turbulence dissipation for different turbulence length scales.

The turbulent kinetic energy inlet profile was generated by fitting a power curve profile to the same set of data recorded for the velocity profile and described in Equation 18. A corresponding turbulence dissipation profile of the same form as the turbulent kinetic energy was obtained using Equation 6 and shown in Equation 19.

$$k = G_k y_w^{-q_k} \tag{18}$$

$$\varepsilon = G_\varepsilon y_w^{-q_\varepsilon} \tag{19}$$

Where constant G_k = 0.0002 and constant q_k = 0.346. Constants G_ε and q_ε are shown in Table 2 for the different turbulence length scales used.

Figure 1 shows the inlet profiles of turbulence intensity, turbulent kinetic energy and turbulence dissipation. It can be seen in Figure 1 (c) that increasing the turbulence length scale reduces the turbulence dissipation.

TABLE 2
EQUATION CONSTANTS FOR TURBULENCE DISSIPATION INLET PROFILE WITH DIFFERENT TURBULENT LENGTH SCALES

Case	**Turbulent Length Scale**		**Equation for Epsilon Inlet Profile**	
	Description	Numerical value (m)	G_ε	q_ε
a	$\ell_{d/3}$	0.1	$4.00\text{x}10^{-6}$	0.519
b	ℓ_d	0.3	$1.00\text{x}10^{-6}$	0.519
c	$\ell_{w/2}$	0.685	$6.00\text{x}10^{-7}$	0.519
d	ℓ_w	1.37	$3.00\text{x}10^{-7}$	0.519
e	$\ell_{f=d}$	f = 0.3	$3.00\text{x}10^{-6}$	1.235
f	$\ell_{f=w/2}$	f = 0.685	$2.00\text{x}10^{-6}$	1.391

D. *Boundary Conditions*

The modelled domain is shown in Figure 3 including the disc location and principle dimensions. The boundary conditions used for each of the domain boundaries are shown in Table 3. A symmetry plane was used to reduce the mesh size, thus reducing computing times.

E. *Mesh Independence*

A structured hexahedral mesh was generated using Gmsh 2.5 finite element grid generator [12]. A coarse mesh containing ~291,000 cells was developed. The mesh was refined using a mesh refinement factor of 1.5 creating two further meshes of ~1,057,000 cells and ~3,763,000 cells. A cross-section of the medium mesh is shown in Figure 2.

TABLE 3
MODEL BOUNDARY CONDITION

Boundary	**Boundary Condition**			
	U	***p***	***k***	***ε***
Inlet	Inlet profile	Zero gradient	Inlet profile	Inlet profile
Outlet	Zero gradient	Fixed value	Zero gradient	Zero gradient
Symmetry Plane	Symmetry plane	Symmetry plane	Symmetry plane	Symmetry plane
Bed	Zero velocity wall	Zero gradient	Wall function	Wall function
Side Wall	Zero velocity wall	Zero gradient	Wall function	Wall function
Surface	Free slip wall	Free slip wall	Free slip wall	Free slip wall

Simulations were run on each of the meshes using the same parameters for both the empty flume and with the disc present. The results were plotted on top of each other to demonstrate the mesh independent solution. It can be seen in Figure 4 that results from the three meshes are almost indistinguishable from one another. This is seen in both the flume and disc results. Therefore for computational efficiency the medium mesh was used for all other simulations. The specified value for the thrust coefficient was 0.86. The model thrust coefficients for course to fine mesh were 0.812, 0.862, and 0.821 which indicates that there is oscillatory convergence. However, the velocity results have been shown to be independent from the mesh on which the simulations were run.

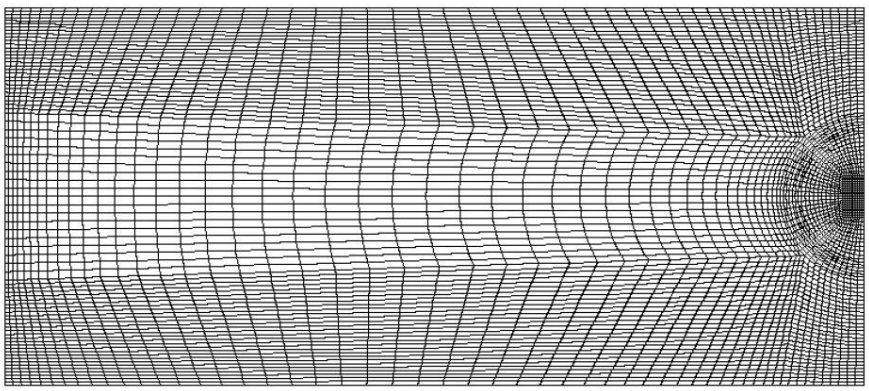

Figure 2 - Medium mesh on y-z plane showing disc to the right

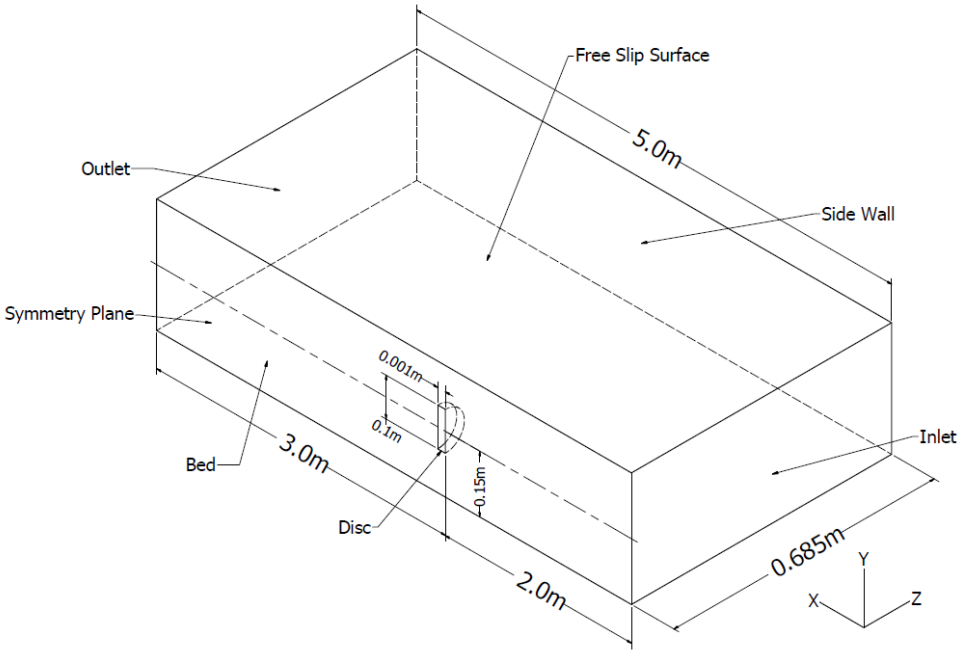

Figure 3 - Flow domain showing principle dimensions.

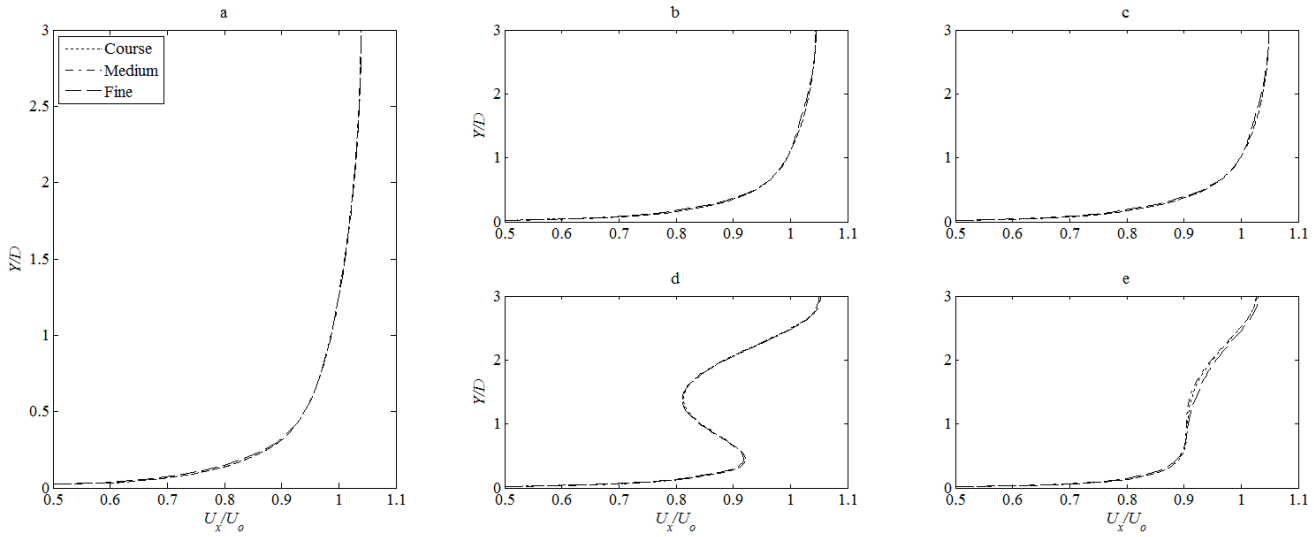

Figure 4 - Mesh Independence. a, b, and c are the flume results, d and e are the disc results. a is 5 diameters upstream of the disc position, b and d are 4 diameters downstream of the disc position, c and e are 11 diameters downstream of the disc position.

IV. Results and Discussion

Velocities have been normalised using the average velocity over the range $0.5 < Y/D < 2.5$: 0.329 m/s for the experiment and 0.333 m/s for the CFD model. Velocities were averaged over this range as this is the range of experimental data.

For analysing the fit between the model results and flume data the parameter $(1 - r^2)$ was used where r is the sum of errors squared and calculated using Equation 20.

$$r = \sum_{1}^{n} \left(y_m - y_{exp}\right)^2 \tag{20}$$

Where n is the number of data points, y_m is the model value and y_{exp} is the experimental value.

A. *Ambient Channel Without Disc*

Figure 5 shows how the vertical velocity profiles compare to experimental data for the different turbulence length scales chosen. It can be seen that the differences between the inlet conditions are subtle, but there are some variations between them. For example, the profiles for a

length scale using Equation 7 and *f=0.685 m*, Figure 5(f), has a smoother transition from boundary to free stream than a length scale of one third the channel depth Figure 5 (a). This, in turn, has a slightly smoother transition from boundary layer to free stream than a length scale of the channel depth, Figure 5(b). The profiles obtained for length scales of half channel width, Figure 5(c), and channel width, Figure 5(d), have a jagged shape rather than a smooth profile as expected. This has been caused by oscillations in the solution.

A possible cause for the instability seen in the solutions for length scales of half channel width and channel width could result from an imbalance of turbulence production and turbulence dissipation terms. The turbulence dissipation term is inversely proportional to the turbulence length scale. Therefore as the length scale increases, turbulence dissipation decreases but the turbulence production/kinetic energy remains the same. Therefore it seems likely that above a length scale of half channel width the difference between turbulence production and dissipation becomes significant causing the solution to become unstable. With further investigation of the solver parameters it may be possible to obtain a stable solution for these length scales.

Five diameters upstream the best fit is seen for a length scale of the channel depth with a $1\text{-}r^2$ value of 0.99772. However, eleven diameters downstream the best fit is seen with length scales of half the channel width and the channel width. However, as previously mentioned these solutions are unstable and not realistic solutions. The next best fit from a stable solution was using a length scale of one third the channel depth which resulted in a $1\text{-}r^2$ of 0.98717.

Investigating the turbulence intensity shows a similar pattern for the length scales of half channel width and channel width. In Figure 6 it can be seen that the plots for half channel width and channel width Figure 6(c & d) contain odd jagged features indicating the solutions are unstable.

It can be seen that changing the length scale has a larger effect on the turbulence intensity than the velocity profiles. Increasing the length scale from one third channel depth to the channel depth caused the turbulence intensity to increase. This is to be expected as increasing the length scale reduces the turbulence dissipation, so the turbulence will increase.

However, the opposite is seen for the length scales calculated from Equation 7. Increasing the length, *f*, from the channel depth to half the channel width causes a reduction in turbulence intensity. The cause of this is the term $(1\text{-}y/f)$ in Equation 7. Close to the surface, $y \rightarrow 0.3m$, this term becomes zero for $f=0.3m$, the channel depth. The length scale will therefore increase resulting in the turbulence dissipation decreasing, causing the turbulence intensity to increase near the surface. For larger values of *f* this term remains non zero which acts to reduce the length scale, increasing turbulence dissipation, thus decreasing the turbulence intensity.

Comparing the turbulence intensity five diameters upstream of the disc position, Figure 6(i), it can be seen that the profile obtained for a length scale of one third the channel depth, Figure 6(a), shows the best agreement with the experimental data with a $1\text{-}r^2$ value of 0.99982. Eleven diameters downstream there is still good agreement with a length scale of one third the channel depth with a $1\text{-}r^2$ of 0.99958.

Overall the best fit has been achieved using a length scale of one third the channel depth. This length scale was used to perform the simulations using an actuator disc in the next section.

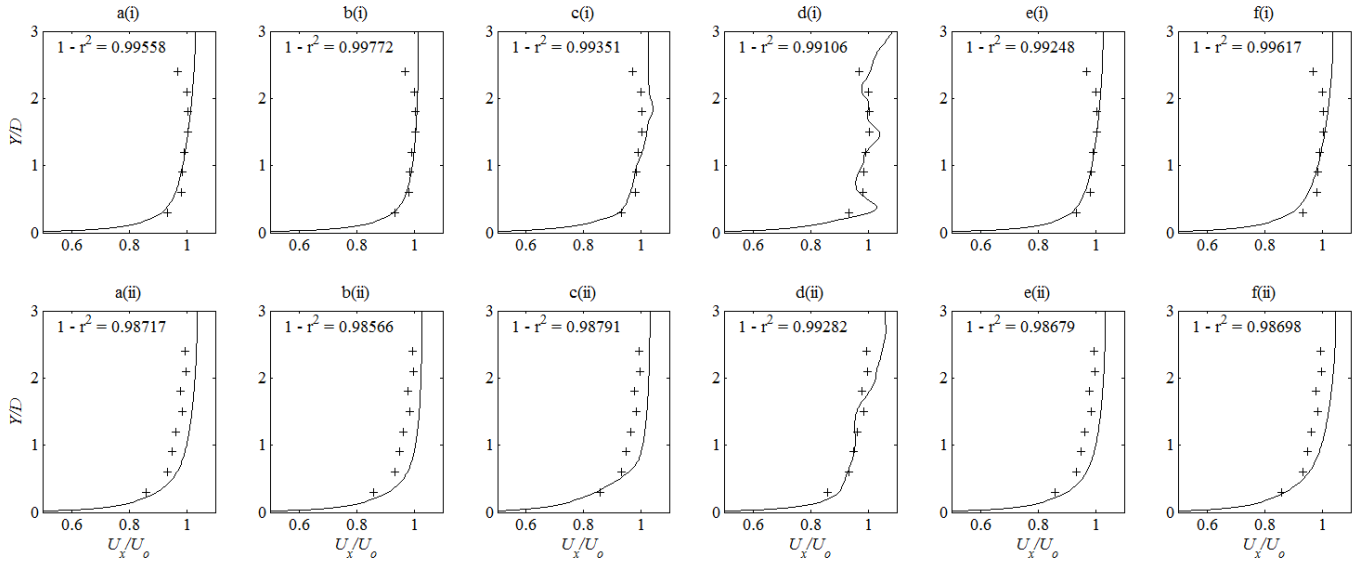

Figure 5 - Flume velocity profiles. (i) 5 diameters upstream of disc position, (ii) 11 diameters downstream of disc position.
a - $\ell_{d/3}$, b - ℓ_d, c - $\ell_{w/2}$, d - ℓ_w, e - $\ell_{f=d}$, f - $\ell_{f=w/2}$

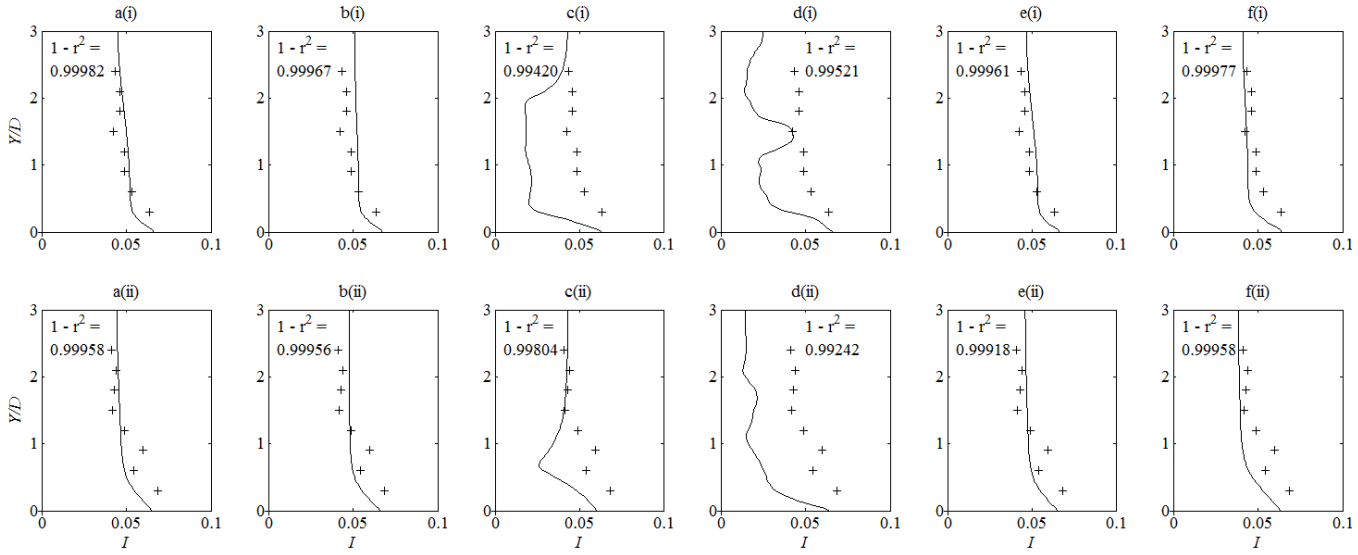

Figure 6 - Flume turbulence intensity. (i) 5 diameters upstream of disc position, (ii) 11 diameters downstream of disc position.
a - $\ell_{d/3}$, b - ℓ_d, c - ℓ_w, d - $\ell_{w/2}$, e - $\ell_{f=d}$, f - $\ell_{f=w/2}$

B. *Actuator Disc Results*

It is to be expected that the results obtained without a turbulence source at the disc will show poorer agreement with the experimental data due to the exclusion of an increase in turbulence caused by the disc. This can be seen in Figure 7(a) where the results from the simulation without an added turbulence source underestimates the velocity deficit and the wake recovery is much faster than measured in the experiments. Using a turbulent length scale of the disc hole diameter, 5 mm, shows the best agreement with the experimental data for the centreline velocity, Figure 7(a). Using a length of half the disc hole diameter, 2.5 mm, results in a larger value of turbulence dissipation and therefore reduces the turbulence in the wake. This reduces the mixing and slows the wake recovery as seen in Figure 7(a).

This is also seen in the turbulence intensity results. For 2.5mm the turbulence intensity is reduced in the wake when compared to a length of 5mm. However, the turbulence intensity drops rapidly for both cases with a turbulence source. There is better agreement without the source added. It is mentioned in the literature [9] that the empirical expression to calculate the maximum turbulence intensity for a turbine should only be used as a starting point. Therefore it is possible that the turbulence set at the disc is an under estimate of what is actually present.

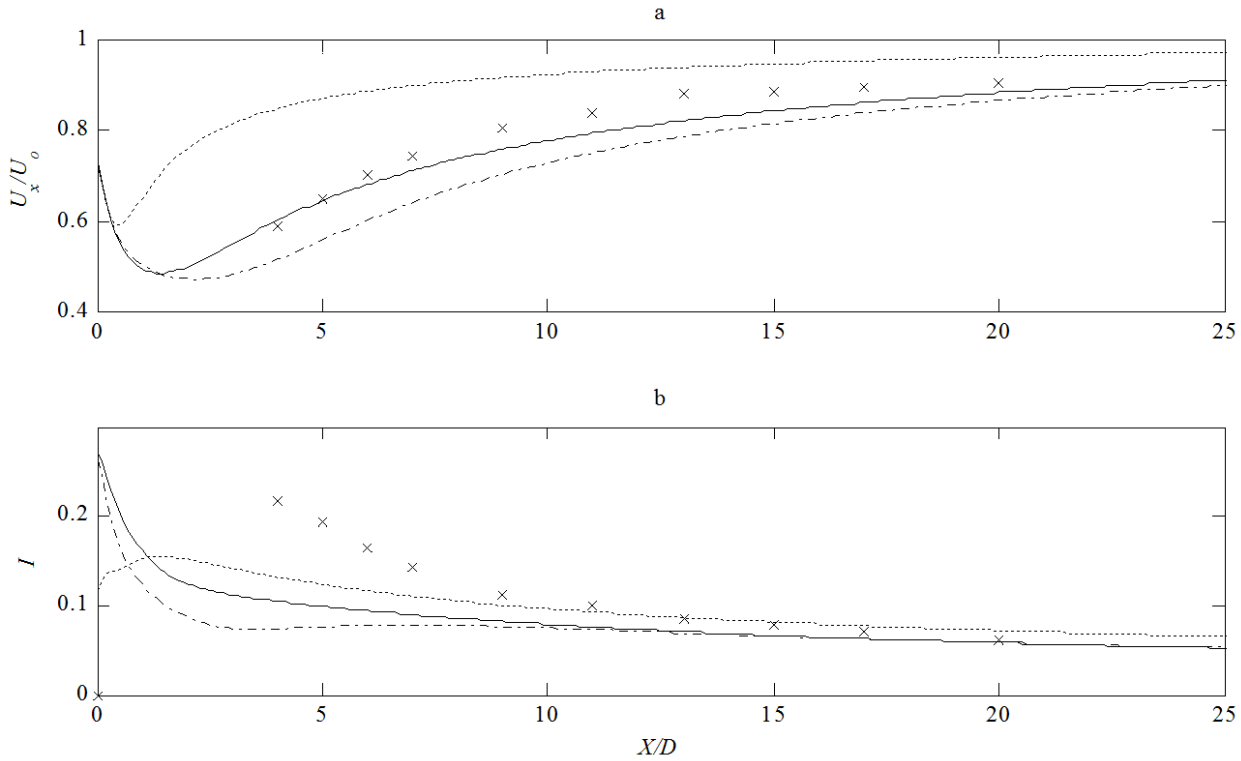

Figure 7 – Centreline velocity (a) and turbulence intensity (b) profiles for three disc turbulence source values:

Solid line – no added turbulence, **Dotted line** - ℓ_i = hole diameter = 5mm, **Dashed line** - ℓ_i = half hole diameter = 2.5mm.

The vertical velocity profiles, Figure 8, show that the model without an added source term under predicts the velocity deficit in the wake. A length scale of 5mm for the turbulence source results in a very good agreement with the experimental data for the velocity profile. However, the turbulence is still under predicted in the near wake and the model without an added source term shows closer agreement. This seems counterintuitive that the turbulence is reduced when a turbulence source is included. However, it can be seen in Figure 7(b) that the inclusion of a turbulence source increase the turbulence intensity at the disc which then rapidly decays to values close to those recorded experimentally in the far wake. Increasing the value of turbulent kinetic energy at the disc will improve the agreement in the near wake, while increasing the turbulence dissipation will damp this increase in turbulent kinetic energy to give good agreement in the far wake. Further investigation is required to find out what these values should be to give the best agreement.

Taking into account the experimental uncertainty of turbulence intensity readings from an ADV and the assumption of uniform momentum and turbulence sources, the model agreement is acceptable and an improvement over previous studies [7].

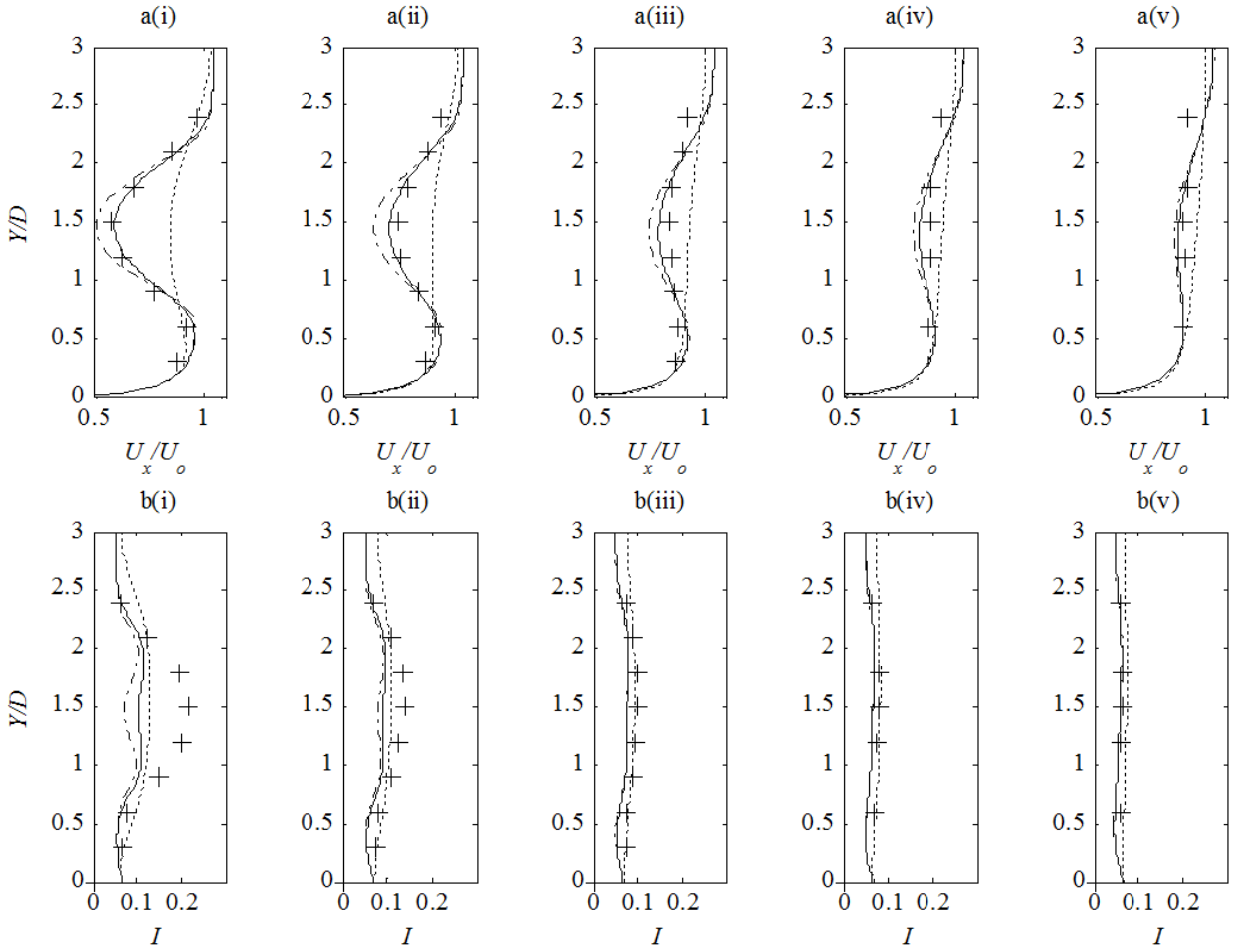

Figure 8 - Vertical velocity (a) and turbulence intensity (b) profiles for different turbulence source values.

Solid line – no added turbulence, **Dotted line** - ℓ_i = hole diameter = 5mm, **Dashed line** - ℓ_i = half hole diameter = 2.5mm.

i) 4 diameters downstream of disc; ii) 7 diameters downstream of disc; iii) 11 diameters downstream of disc; iv) 15 diameters downstream of disc; v) 20 diameters downstream of disc.

V. CONCLUSIONS

It has been shown that the length scale affects the results of actuator disc RANS models for predicting the wake of horizontal axis tidal stream turbines. Varying the length scale had a more significant effect on turbulence intensity profiles than the velocity results. For this study a length scale of one third the channel depth to define the inlet turbulence dissipation showed the best agreement to experimental data. However, further investigation is required to demonstrate that this is the case for other flow scenarios.

Adding a turbulence source term to the actuator disc significantly improved the agreement between the velocity profiles of the model and experiments. The length scale that showed the best agreement was the diameter of the holes used on the porous disc for experiments. However, the agreement with the turbulence intensity was reduced at this length scale. A possible explanation is that the turbulence intensity at the disc was underestimated. Therefore further investigations are required with larger values of the turbulent kinetic energy at the disc.

VI. FURTHER WORK

More experimental data is required over a wider range of flow conditions to allow broader conclusions to be drawn.

Further investigation of the turbulence intensity at the disc is required to improve agreement with experimental data.

To provide a better understanding of what length scales are present, experimental data is required to enable actual values to be set in the model.

REFERENCES

[1] T. Burton, D. Sharpe, N. Jenkins, and E. Bossanyi, Wind energy handbook. 2001: *Wiley*.

[2] R. Mikkelsen, "Actuator disc methods applied to wind turbines", Doctor of Philosophy Thesis, Technical University of Denmark, 2003.

[3] H.K. Versteeg and W. Malalasekera, An introduction to Computational Fluid Dynamics: The finite volume method. 1995: *Longman Scientific & Technical*.

[4] X. Sun, "Numerical and Experimental Investigation of Tidal Current Energy Extraction", Doctor of Philosophy Thesis, The University of Endinburgh, 2008.

[5] A.J. MacLeod, S. Barnes, K.G. Rados, and I.G. Bryden. Wake effects in tidal current turbine farms. in *MAREC Conference*. 2002. Newcastle.

[6] L.E. Myers and A.S. Bahaj, Experimental analysis of the flow field around horizontal axis tidal turbines by use of scale mesh disk rotor simulators. *Ocean Engineering*, 2010. 37(2-3): p. 218-227.

[7] M.E. Harrison, W.M.J. Batten, L.E. Myers, and A.S. Bahaj, Comparison between CFD simulations and experiments for predicting the far wake of horizontal axis tidal turbines. *IET Renewable Power Generation*, 2010. 4(6): p. 613-627.

[8] T. Roc, D.C. Conley, and D. Greaves, Accounting for turbulence in a regional numerical model for tidal current turbine farm planning, in *3rd International Conference on Ocean Energy*. 2010: Bilbao.

[9] A. Crespo and J. Hernandez, Turbulence characteristics in wind-turbine wakes. *Journal of Wind Engineering and Industrial Aerodynamics*, 1996. 61: p. 71-85.

[10] OpenFOAM, The Open Source CFD Toolbox: User Guide. Version 1.7.1. 2010.

[11] OpenFOAM, The Open Source CFD Toolbox: Programmer's Guide. Version 1.7.1. 2010.

[12] C. Geuzaine and J.-F. Remacle. Gmsh Reference Manual for Gmsh 2.5. 2010 [cited May 2011]; Available from: http://www.geuz.org/gmsh.